PHYSICAL REVIEW B VOLUME 12, NUMBER 4 15 AUGUST 1975

Crystallographic, elastic, and Raman scattering investigations of structural phase transitions in $RbCdF_3$ and $TlCdF_3$

M. Rousseau, J. Y. Gesland, J. Julliard, and J. Nouet
Laboratoire de Physique de l'Etat Condensé, Faculté des Sciences, Route de Laval, 72000 Le Mans Cedex 72017, France

J. Zarembowitch
Laboratoire de Chimie de Coordination, E.N.S.C.P. 11, rue Pierre et Marie Curie, Paris

A. Zarembowitch
Laboratoire de Recherches Physiques, Université Pierre et Marie Curie, 75230 Paris Cedex 05, France*

(Received 5 May 1975)

A simple model of force constants allowed us to forecast that structural phase transitions due to MF_6 octahedra rotations may occur in the fluoperovskites AMF_3 containing M ions large enough to determine the dimensions of the cell and leave the A ions free to move from the octahedra. Thus we focused our attention on $ACdF_3$ compounds. We successfully prepared large single crystals of $RbCdF_3$, $TlCdF_3$, and $CsCdF_3$ by the Bridgman-Stockbarger method. These crystals have the cubic perovskite structure at room temperature. The x-ray experiments show that a tetragonal distortion with $c/a > 1$ occurs at 124 K in $RbCdF_3$ and 191 K in $TlCdF_3$. For $CsCdF_3$, no distortion was observed between 4 and 300 K. The occurence of a phase transition in $RbCdF_3$ and $TlCdF_3$ has been confirmed by the study of elastic wave velocities as a function of temperature. The anomalous decreasing of the elastic constant C_{44} with decreasing temperature is consistent with slight rotations of CdF_6 octahedra. The study of both superstructure reflexions and Raman-scattering spectrum allows us to retain the space group D_{4h}^{18} for the low-temperature phase. Two low-frequency modes show a behavior of soft modes very similar to that already observed in $SrTiO_3$ and $KMnF_3$.

I. INTRODUCTION

Over the last few years, much work has been devoted to the experimental and theoretical study of structural phase transitions occuring in some compounds of perovskite structure such as $SrTiO_3$, $LaAlO_3$, $NaNbO_3$, $KMnF_3$, $CsPbCl_3$, $CsPbBr_3$, etc. Both EPR, x-ray scattering, neutron scattering, and Brillouin scattering experiments have shown that these transitions are associated with soft modes at M, R, or X points of the cubic Brillouin zone.[1-3] A thorough study of the mechanism of these transitions requires a knowledge of the microscopic force constants in these materials. In the main works published so far, the parameters of the interaction Hamiltonian are determined by fitting, for instance, the theoretical curves of phonon dispersion with the experimental curves, for a given material. This approach gives very good punctual results but it does not allow us to give an answer to the fundamental question: Why do structural phase transitions occur or not in compounds of perovskite structure?

The study of sequences of isotype compounds among which some present phase transitions is a way of tackling this problem. This is why we have focused our attention on the AMF_3 compounds (where A is a monovalent ion and M a divalent ion) which offer a wide range of insulating materials of perovskite structure, whose properties are closely linked to the choice of the A and M ions.

The organization of the present paper is as follows. In Sec. II, we show how a simple model of force constants which, when applied to one single compound would yield insignificant information, can lead to interesting qualitative results in the study of a sequence of materials. This model allows us to consider the possible existence of phase transitions due to rotations of MF_6 octahedra in the AMF_3 compounds for which the dimensions of the cubic unit cell are essentially determined by the M– F bonds. In order to study these transitions, we have focused our attention on the $ACdF_3$ sequence[4] (A = K, Rb, Tl, Cs) in which we expect to find the existence of a change of phase for $KCdF_3$, $RbCdF_3$, and $TlCdF_3$. The method of growth that allowed us to obtain large single crystals is described in Sec. III. Just as expected, the radiocrystallographic study (Sec. IV) reveals the existence, at low temperature, of a quadratic distortion in $RbCdF_3$ and $TlCdF_3$. No distortion is observed in $CsCdF_3$. Besides, $KCdF_3$ that is already distorted at room temperature, will be studied at a further stage. The determination on single crystal of ultrasonic wave velocities in function of the temperature (Sec. V) has allowed us to follow the evolution of the force constants and to confirm the hypothesis of the rotation of the MF_6 octahedra around the ⟨100⟩ axes. So, according to Glazer,[5] only the D_{4h}^5 and the D_{4h}^{18} space groups have to be considered for the quadratic phase. As predicted by group theory, the results of Raman scattering described in Sec. VI show the presence of lines characteristic of the D_{4h}^{18} group. Section VII is a summary and brief description of related work in progress.

II. MODEL OF FORCE CONSTANTS

A. Parameters of the model

The fluoperovskites of general formula $AM\mathrm{F}_3$, where A is a monovalent atom, M a divalent atom, and F the fluorine (Fig. 1), are mainly ionic in character. Thus the crystal stability is assumed by electrostatic long-range interactions and by short-range overlap interactions. In our model, the short-range potential energy of the crystal bulk is assumed to be a sum of two bodies axially symmetric interactions limited to second neighbors. Then, for each type of short-range interaction, two parameters are needed to specify axially symmetric forces. These parameters were chosen to be the second derivative of the short-range potential function V_i, parallel and perpendicular to the line joining the interacting ions. These parameters are specified by

$$A_i = \frac{2v}{e^2}\left(\frac{\partial^2 V_i}{\partial r_{i\parallel}^2}\right)_{\mathrm{equ}}, \quad B_i = \frac{2v}{e^2}\left(\frac{\partial^2 V_i}{\partial r_{i\perp}^2}\right)_{\mathrm{equ}},$$

where v is the volume of the unit cell; the suffix i is 1 for A–F, 2 for M–F and 3 for F–F interactions. Our purpose consists mainly in obtaining qualitative information which would allow us to compare various compounds. In order to minimize the number of parameters, we have used the following assumptions: The ionic charges are supposed to be integers

$$Z_A = 1, \quad Z_M = 2, \quad Z_{\mathrm{F}} = -1 .$$

A calculation of the six coefficients A_i and B_i has been made by Cowley *et al.*[6] for $\mathrm{SrTiO_3}$ by fitting the experimental dispersion curves. On the basis of these results, it can be seen that B_1, A_3, and B_3 are small compared to A_1, A_2, and B_2; so we neglect them.

Under these assumptions, the elastic constants (Ref. 7) C_{11}, C_{12}, and C_{44} can be expressed by

$$C_{11} = (e^2/rv)[\tfrac{1}{8}(2A_1 + A_2) - 6.185] ,$$

$$C_{12} = (e^2/rv)[\tfrac{1}{8}(A_1 - B_2) - 1.033] ,$$

$$C_{44} = (e^2/rv)[\tfrac{1}{8}(A_1 + B_2) + 3.093] .$$

The technique for growing single crystals described in Sec. III of the present paper gave us single crystals large enough to determine the elastic constants of many perovskite fluorides[8] by ultrasonic methods. The experimental data and the force constants derived from them are listed in Table I.

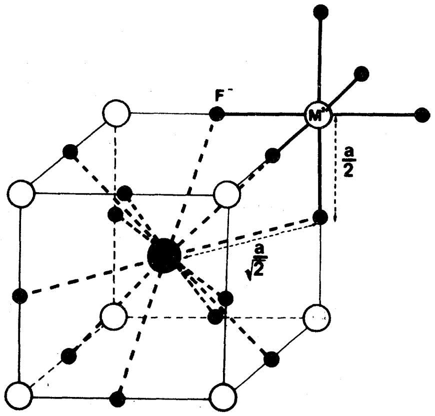

FIG. 1. Cubic perovskite crystal structure.

B. Study of force constants

In the harmonic approximation, we determined the potential energy variations when an ion is displaced from its equilibrium position. Contrary to A and M ions taking place in cubic symmetry sites, the F ions are located in sites of symmetry D_{4h}; so we must distinguish the displacements perpendicular to the direction F–M–F from the displacements parallel to this direction (Fig. 2).

Thus we have established that displacements x_A, x_M, $x_{\mathrm{F}\parallel}$, and $x_{\mathrm{F}\perp}$ induce, respectively, energy variations dV_A, dV_M, $dV_{\mathrm{F}\parallel}$, and $dV_{\mathrm{F}\perp}$, given by

$$dV_A = (e^2/2v)(2A_1 - 16\beta_A)x_A^2 ,$$

$$dV_M = (e^2/2v)(A_2 + 2B_2 - 16\beta_M)x_M^2 ,$$

$$dV_{\mathrm{F}\parallel} = (e^2/2v)(A_2 - 16\beta_{\mathrm{F}\parallel})x_{\mathrm{F}\parallel}^2 ,$$

$$dV_{\mathrm{F}\perp} = (e^2/2v)(A_1 + B_2 - 16\beta_{\mathrm{F}\perp})x_{\mathrm{F}\perp}^2 .$$

The coefficients β_A, β_M, $\beta_{\mathrm{F}\parallel}$, and $\beta_{\mathrm{F}\perp}$ characterizing electrostatic energy are calculated in the Appendix.

Then, the harmonic force constants are expressed by

$$k_A = (e^2/2v) \times 4A_1, \quad k_M = (e^2/2v)(2A_2 + 4B_2) ,$$

$$k_{\mathrm{F}\parallel} = (e^2/2v)(2A_2 - 85.66) ,$$

$$k_{\mathrm{F}\perp} = (e^2/2v)(2A_1 + 2B_2 + 42.83) .$$

The numerical results are listed in Table I.

C. Phase transitions

Let us compare the force constant k_{F} with the coefficient $\Delta r_{A\mathrm{F}}$ defined by

TABLE I. Force constants of some fluoperovskites.

	$KMgF_3$	$KNiF_3$	$KZnF_3$	$KCoF_3$	$KMnF_3$	$RbCoF_3$	$RbMnF_3$
a (Å)	3.973	4.010	4.054	4.069	4.190	4.127	4.239
K_A (10^4 erg cm^{-2})	7.95	8.37	9.0	8.56	5.96	10.57	7.57
K_M (10^4 erg cm^{-2})	20.53	21.61	16.17	15.68	16.28	13.95	15.51
$K_{F\parallel}$ (10^4 erg cm^{-2})	15.51	19.38	15.12	15.12	15.26	13.02	14.28
$K_{F\perp}$ (10^4 erg cm^{-2})	6.48	5.30	5.03	4.56	3.49	5.75	4.40
Δr_{AF} (Å)	−0.054	−0.035	−0.013	−0.006	+0.055	−0.068	−0.012

$$\Delta r_{AF} = \tfrac{1}{2}a - (r_A + r_F)/\sqrt{2} .$$

r_A and r_F are the ionic radii tabulated by Shanon and Prewitt.[9]

We can say ingenuously that a positive value of this coefficient might lead to a possibility of motion of the A sublattice with respect to the F sublattice, whereas a negative value indicates a close packing of A and F ions. In addition, $k_{F\perp}$ being much smaller than $k_{F\parallel}$, we can conclude that $x_{F\perp}$ displacements corresponding to rotations of MF_6 octahedra are probable when Δr_{AF} is positive. In fact, looking at Table I, we can see that $KMnF_3$ for which Δr_{AF} is positive is the only compound presenting a structural phase transition. By the way, we may note that $k_{F\perp}$ decreases as Δr_{AF} increases.

Thus, we may expect that a structural phase transition due to rotations of MF_6 octahedra may occur in those fluoperovskites where the lattice parameter a is greater than $(r_A + r_F)\sqrt{2}$. In practice, this configuration is obtained in the AMF_3 compounds containing M ions large enough to determine the dimension of the cell and leave the A ions free to move from the octahedra.

In order to study over a large range of compounds the phenomena due to octahedra rotations, we focused our attention on the diamagnetic fluoperovskites $ACdF_3$. According to Table II, we should expect to observe structural phase transition in $RbCdF_3$ and $TlCdF_3$ for which Δr_{AF} is largely positive.

III. CRYSTAL PREPARATION

The samples were prepared by direct reaction of purified fluorides in a sealed platinum crucible. The high-purity powders of RbF, CsF, or TlF and CdF_2 were accurately weighed in a dry box and mixed in stoichiometric proportions. The mixtures of approximately 200 g were inserted in a conical bottomed platinum crucible. To prevent moisture and oxygen contamination, the container was heated to 150℃ while connected to a high vacuum line, then it was welded shut and heated to approximately 50℃ above the melting point of the mixture. Single crystals were grown by the Bridgman-Stockbarger technique: the crucible was lowered in a vertical furnace through a temperature gradient of 8℃/cm at rates of 15–20 mm per 24 h.

From each large polycrystalline ingot, we can obtain two or three single crystals of good optical quality measuring to the order of 1–1.5 cm³. The crystals were oriented by the x-ray Laue back reflection and cut with flat and parallel faces either perpendicular to the ⟨100⟩ fourfold axes or to the [001], [110] axes or to the [111], [1$\bar{1}$0] axes. For example, the dimensions of two differ-

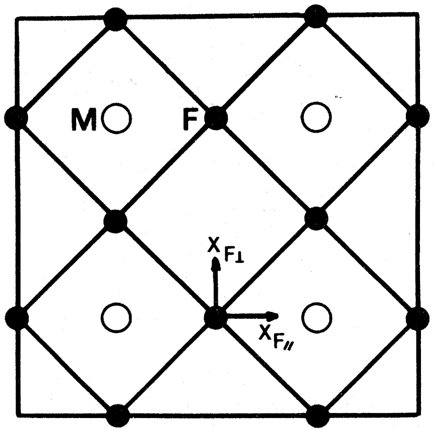

FIG. 2. (100) plane containing M^{++} ions. $x_{F\parallel}$ and $x_{F\perp}$ represent displacements of F ions parallel and perpendicular to the F–M–F direction, respectively.

TABLE II. Lattice parameter a, stability coefficient Δr_{AF}, elastic constants C_{11}, C_{12}, C_{44}, and force constants K_A, K_M, $K_{F\parallel}$, $K_{F\perp}$ for $RbCdF_3$, $CsCdF_3$, and $TlCdF_3$ at room temperature.

	a (Å)	Δr_{AF} (Å)	C_{11}	C_{12}	C_{44}	K_A	K_M	$K_{F\parallel}$	$K_{F\perp}$
				10^{11} dyn cm^{-2}			10^4 erg cm^{-2}		
$RbCdF_3$	4.399 ± 0.001	+0.068	10.96 ± 0.02	3.73 ± 0.05	2.04 ± 0.02	5.69	15.10	15.39	2.70
$CsCdF_3$	4.465 ± 0.001	−0.006	10.78 ± 0.02	4.05 ± 0.05	2.50 ± 0.02	7.48	13.2	13.48	3.60
$TlCdF_3$	4.395 ± 0.001	+0.044	10.28 ± 0.06	3.85 ± 0.05	1.77 ± 0.01	5.40	13.42	14.40	2.21

ent samples were 12×9×8 mm, 11×7×6 mm for $RbCdF_3$ and 9×9×5 mm, 8×7×5 mm for $TlCdF_3$.

IV. CRYSTALLOGRAPHIC DATA

Experiments were carried out on a Philips powder x-ray diffractometer with the use of copper radiation. A liquid-helium cryostat[10] allowed us to obtain a stability of temperature better than 0.1 K within, the period of measurements, from 4 to 300 K.

In this range of temperature, we observe no distortion for $CsCdF_3$ (Fig. 3). On the other hand, for $TlCdF_3$ and $RbCdF_3$ we observe a quadratic distortion at low temperatures. In fact, the *hhh* lines are not affected, the *hhl* lines are split into two lines of respective intensity I and $2I$, the *hkl* lines give three lines of equal intensity.

In order to determine T_c accurately, we have studied the temperature dependence of the 521 reflection linewidth. No hysteresis was observed at the transition. Thus we obtain

$$T_c = 124 \pm 1 \text{ K for } RbCdF_3\,,$$

$$T_c = 191 \pm 1 \text{ K for } TlCdF_3\,.$$

We have studied on line 400 the variations of c/a as a function of temperature. Under T_c, the rela-

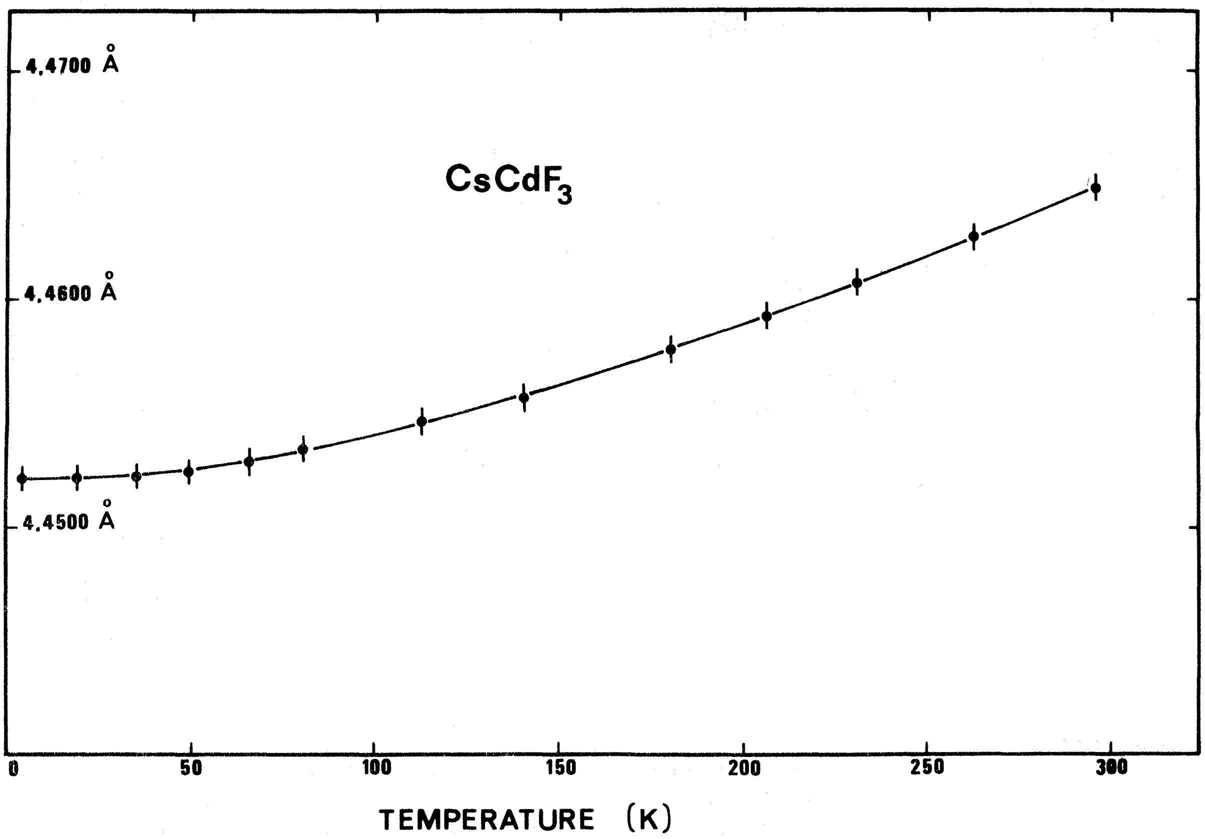

FIG. 3. Temperature dependence of the lattice parameter in $CsCdF_3$.

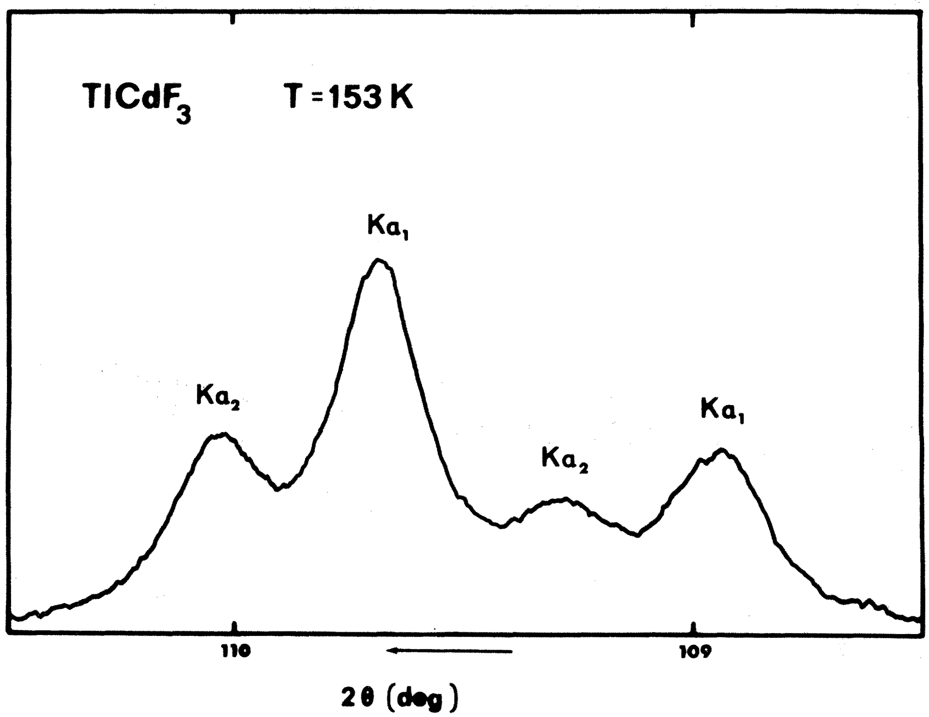

FIG. 4. Recorder chart trace of the 400 pseudocubic Bragg peak at 153 K in TlCdF$_3$.

tive positions of the two lines which come from the 400 line show that c/a is greater than one. For temperatures much smaller than T_c, the two lines are well separated (Fig. 4), but near T_c a graphical analysis is necessary. The temperature dependence of the cubic parameter a_c and the quadratic lattice parameters a and c are shown in Fig. 5 for RbCdF$_3$ and TlCdF$_3$. The distortion is greatest for TlCdF$_3$ and rises to 1.3% at 4.2 K. The lack of hysteresis and volume discontinuity at the transition are compatible with a second-order phase transition.

For determination of the space group of the crystal below T_c, the conditions of extinction for the two space groups D_{4h}^5 and D_{4h}^{18} suggested in Sec. V were analyzed. A systematic search for the superstructure reflections associated with these two groups allowed us to observe only the $\frac{3}{2}\frac{1}{2}\frac{1}{2}$ line corresponding to an R point of the pseudocubic Brillouin zone. Thus, the D_{4h}^{18} space group may be retained for the low-temperature phase.

V. ULTRASONIC WAVE PROPAGATION

A. Experimental results

We have measured the velocities of longitudinal and shear elastic waves both by the ultrasonic pulse superposition and by observing in polarized light the successive ultrasonic resonances of the samples. The measurements were taken on different samples with parallel faces oriented either perpendicular to the [100], [110], or [111] directions. The sample under examination was placed in a cryostat, allowing us to vary the temperature continuously from 10 to 300 K. The temperature homogeneity is assumed by helium gas. Very near the transition, the optical method is not very suitable, due to heating of the crystal by ultrasonic waves. On the other hand, with the pulse superposition technique, a temperature stability of 0.001 K was obtained. Figure 6 shows our results for the different modes. Near the transition, we do not observe a step function for temperature dependence of the velocities as the theory predicted[1] but observe rather a sharp decrease occuring over a few degrees. This is probably due to residual strains in the crystal, which one can visualize with the optical method. All our samples were prepared by the Bridgman-Stokbarger technique described in Sec. III; this method gives large single crystals, but we cannot avoid the occurence of strains. In fact, in order to evaluate, in the temperature dependence of the velocities the part due to coupling between strain and order parameter from the part due mainly to formation of domains and critical fluctuations, further experimental measurements will be necessary.

B. Discussion

Let us compare the temperature dependence of the elastic constant C_{44} in TlCdF$_3$, RbCdF$_3$, and CsCdF$_3$ (Fig. 7). For CsCdF$_3$, in which no phase

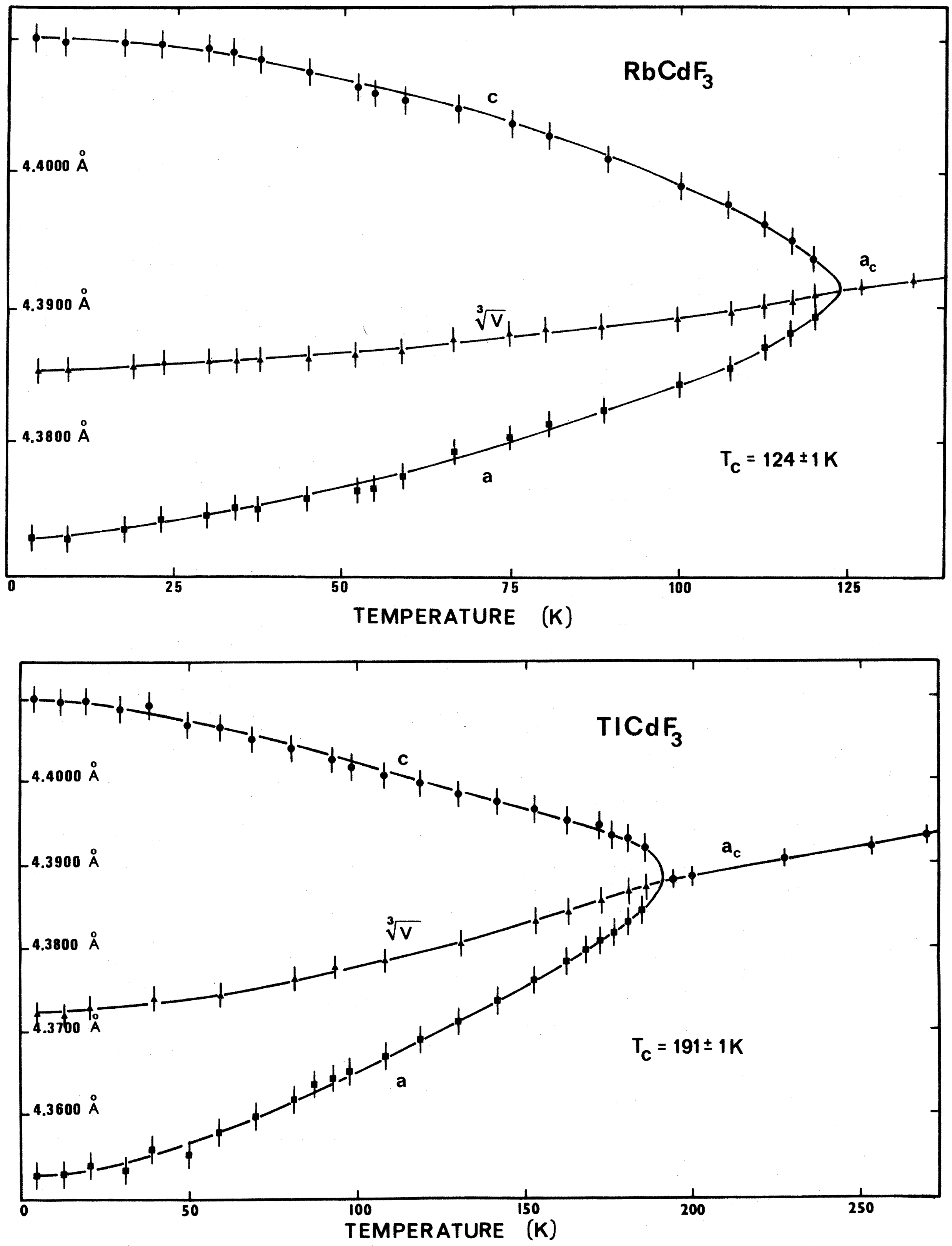

FIG. 5. Lattice parameters vs temperature for (a) RbCdF$_3$ and (b) TlCdF$_3$.

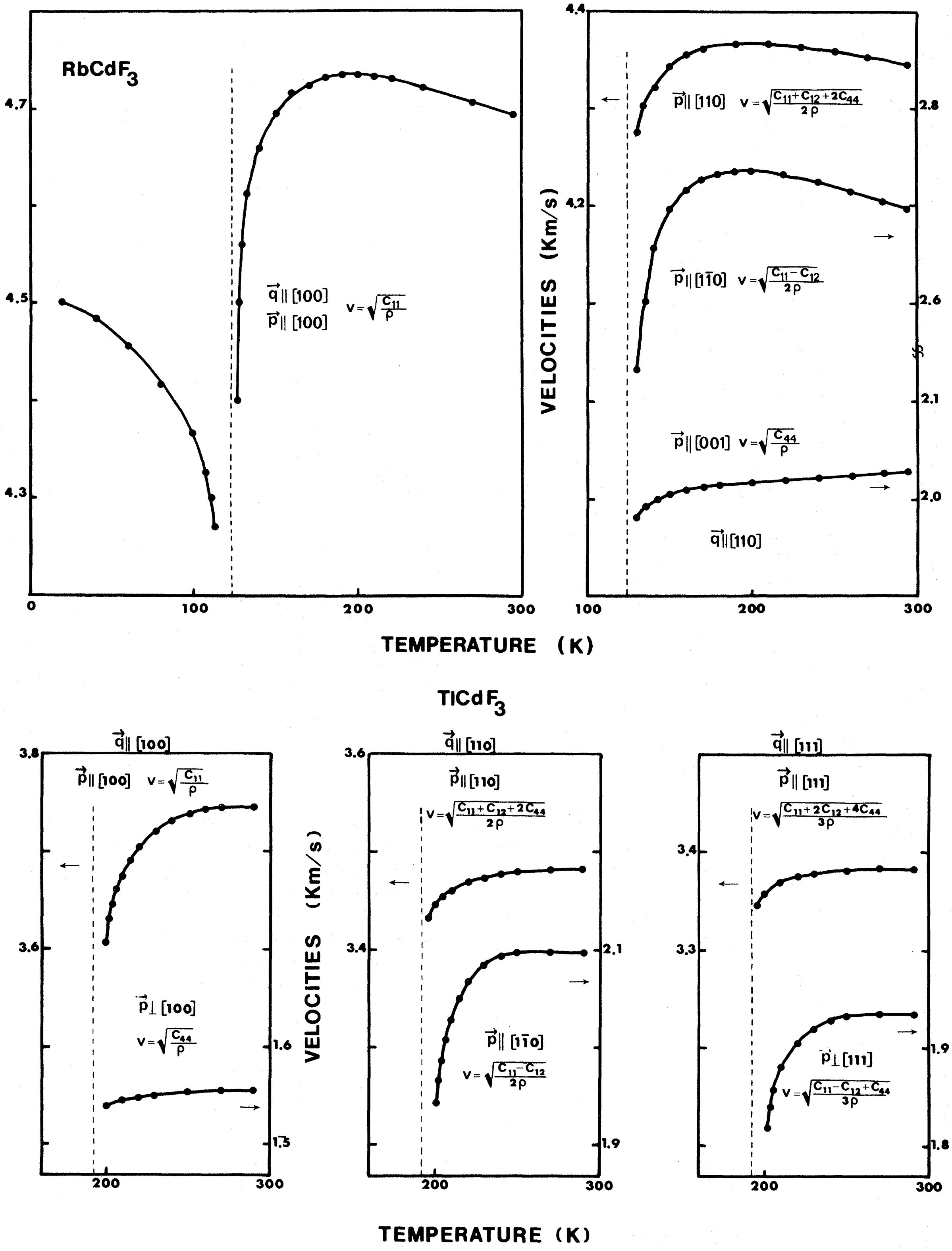

FIG. 6. Velocities for longitudinal and shear waves propagating (a) along the [100] and [110] directions for RbCdF$_3$ (b) and along the [100], [110], and [111] directions for TlCdF$_3$.

transition has been observed; as usual, C_{44} increases as the temperature decreases. On the other hand, for $TlCdF_3$ and $RbCdF_3$ one notes over and above the large variations near the transition a weak increase of C_{44} with temperature. This anomalous behavior may be associated with a soft mode. In fact, with the model described in Sec. II, the elastic constant C_{44} and the restoring force constants $k_{F\perp}$ are expressed by

$$C_{44}=(e^2/rv)[\tfrac{1}{8}(A_1+B_2)+3.093]\,,$$

$$k_{F\perp}=(e^2/2v)(2A_1+2B_2+42.83)\,.$$

Thus, it is clear that a decrease of C_{44} is caused by a softening of this force constant. Owing to the fact that $k_{F\perp}$ is the restoring force constant tending to reduce the rotation of CdF_6 octahedra, we may suppose that the observed distortions are due to such rotation.

Here, it is of great interest to note the unusual fact that in the expression of $k_{F\perp}$, the electrostatic contribution is positive, whereas the overlap contribution is negative. Then, a decrease of $k_{F\perp}$ is due to an increase of A_1+B_2 in absolute value.

Under this assumption, according to Glazer,[5] the two space groups D_{4h}^5 and D_{4h}^{18} have to be considered for the low-temperature phase. In fact, as is shown in Sec. III, the x-ray data display superstructure reflections consistent with the space group $D_{4h}^{18}(I\frac{4}{m}\text{cm})$. Let us see now how these conclusions are backed up by Raman-scattering experiments.

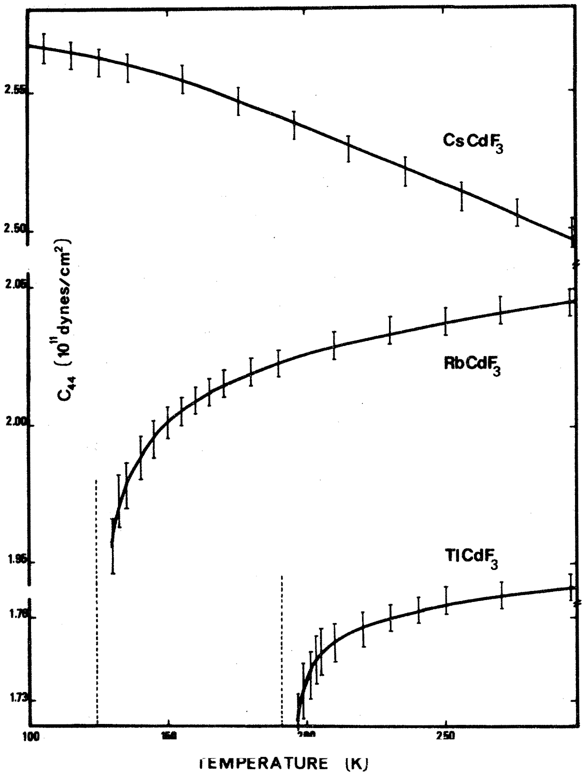

FIG. 7. Temperature variation of the elastic constant C_{44} of $CsCdF_3$, $RbCdF_3$, and $TlCdF_3$.

VI. RAMAN SCATTERING

A. Experiments

The Raman spectra were recorded on a CODERG double monochromator spectrometer. The temperature dependence of the low-frequency soft modes was studied with a CODERG spectrometer including a triple monochromator. The spectra were excited with 800 mW of argon-laser light at 4880 Å; slit widths of 3 to 1 cm^{-1} were used. The investigated samples were cut in the form of parallelepipeds with faces perpendicular to the fourfold cubic axes. The directions x, y, z that are used to denote the various polarizations refer to the crystal cubic axes.

There is no first-order Raman spectrum in the high-temperature cubic phase. In the low-temperature tetragonal phase, four normal modes belonging to the B_{1g}, B_{2g}, A_{1g}, E_g representations are Raman active if the space group is D_{4h}^5; seven modes associated with the $1A_{1g}+3E_g+2B_{1g}+1B_{2g}$ representations are expected if the space group is D_{4h}^{18}. When the crystal is cooled below 191 K for $TlCdF_3$ and 124 K for $RbCdF_3$, seven lines can be observed whose frequencies are listed in Table III.

B. Spectra and assignments

The state of polarization of the Raman lines allows us to assign them to the Raman-active modes in the D_{4h}^{18} space group. The polarized Raman spectra of $RbCdF_3$ and $TlCdF_3$ at 40 K are shown in Fig. 8. It is worth noticing that in spite of the three possible orientations for the tetragonal unit cell relative to the cubic unit cell, the polarization of the lines is well defined.

TABLE III. Peak frequencies (cm^{-1}) for the first-order Raman spectra of $RbCdF_3$ and $TlCdF_3$ at 40 K.

	$RbCdF_3$ (cm^{-1})	$TlCdF_3$ (cm^{-1})
E_g	27	16
A_{1g}	72	101
E_g	78	46
B_{1g}	82	47
–	189	139
B_{1g}	196	153
B_{2g}	324	317

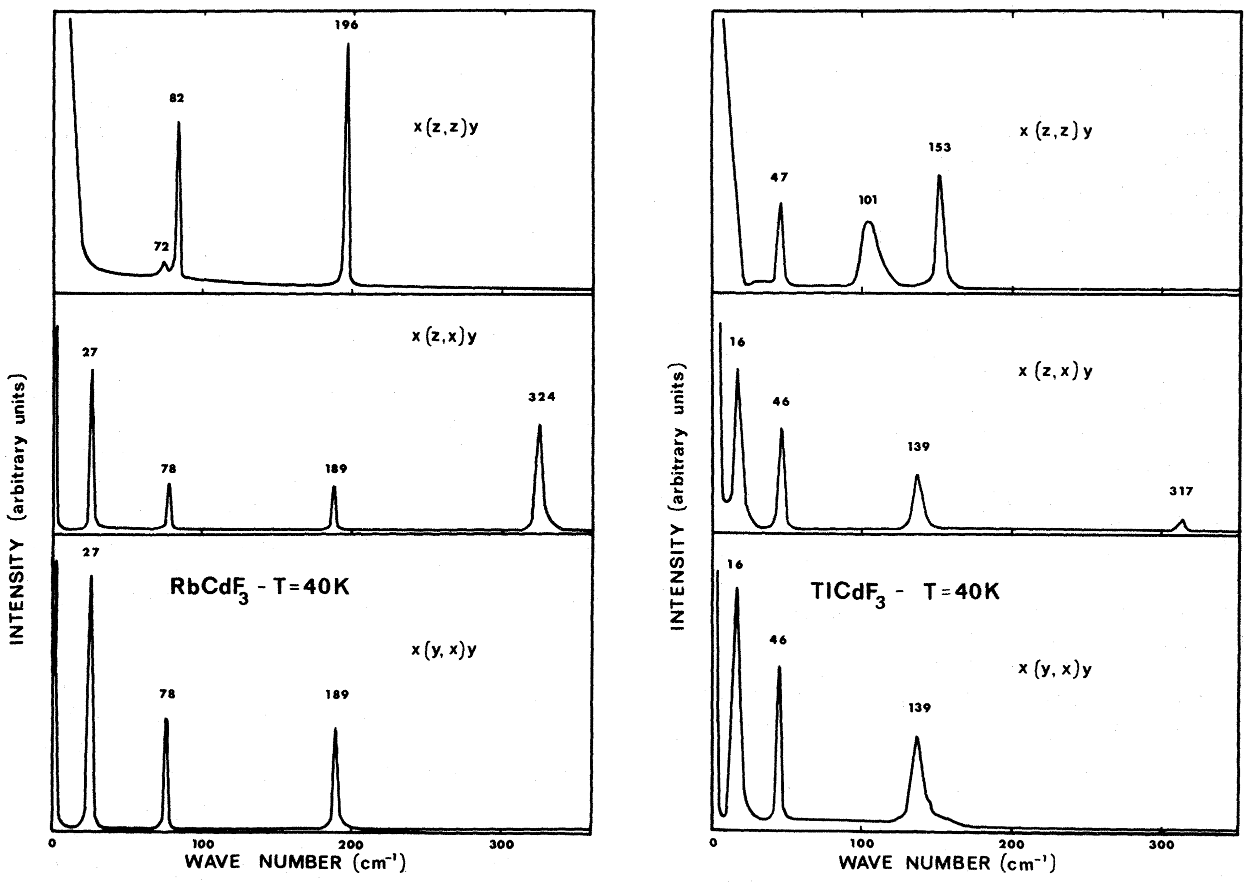

FIG. 8. Polarized Raman spectra of (a) $RbCdF_3$ and (b) $TlCdF_3$ at 40 K. x, y, and z refer to the cubic axes.

In $RbCdF_3$, the 324-cm^{-1} band is intense in the $x(z,x)y$ spectrum. This band cannot be observed in the $x(y,x)y$ spectrum. This implies first, that the tetragonal axis of the domain has a preferred orientation along the ox or oy axis of the cubic cell; secondly, that this frequency must be assigned to the B_{2g} normal mode. On the other hand, the separation between the two bands at 78 cm^{-1} (nondiagonal element of the Raman tensor) and 82 cm^{-1} (diagonal element) vanishes when the temperature approaches 124 K. Thus, the two bands can be assigned to a couple E_g, B_{1g}, due to the removing of degeneracy in the tetragonal phase of a triply degenerate mode at the edge of the cubic phase Brillouin zone. The same conclusion can be drawn with regard to the two peaks at 189 and 196 cm^{-1} which belong to the E_g, B_{1g} species. These observations support the assignment to an E_g mode of the 27 cm^{-1} line, which appears both in the $x(y,x)y$ and $x(z,x)y$ spectra and the attribution to an A_{1g} mode of the 72 cm^{-1} band, which occurs in the $x(z,z)y$ spectra. Similar considerations allow us to assign the seven observed lines in $TlCdF_3$ to the Raman active modes in the D_{4h}^{18} point group.

C. Temperature dependence of the spectra

With respect to the temperature dependence, the behavior of the two compounds is markedly different. In $RbCdF_3$ two modes are upset when the temperature is increased from 40 to 124 K: the A_{1g} mode and the E_g mode of lowest frequency; the latter mode remains underdamped and its frequency decreases from 27 cm^{-1} at 40 K to 10 cm^{-1} at 115 K (Fig. 9). When heating the crystal, the A_{1g} mode (72 cm^{-1} at 40 K) cannot be identified above 95 K (about 60 cm^{-1} at 90 K). In $TlCdF_3$ too, the corresponding E_g and A_{1g} lines are also the most strongly influenced by the transition. However, due to its widening, the E_g line (16 cm^{-1} at 40 K), well resolved at this temperature, is no longer separate from the Rayleigh line for $T > 90K$, unless its frequency is slightly affected (Fig. 10). At 100 K, this line is overdamped and it cannot be distinguished from the Rayleigh line. In the same way, as can be seen in Fig. 11, the A_{1g} line whose frequency varies from 101 cm^{-1} at 40 K to 75 cm^{-1} at 110 K is much wider.

This temperature dependence is very similar to

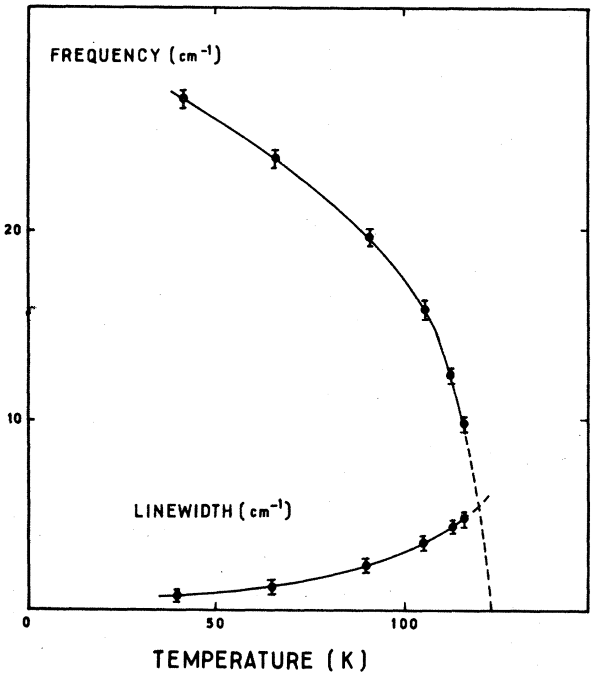

FIG. 9. Temperature dependence of the soft phonon mode E_g in $RbCdF_3$.

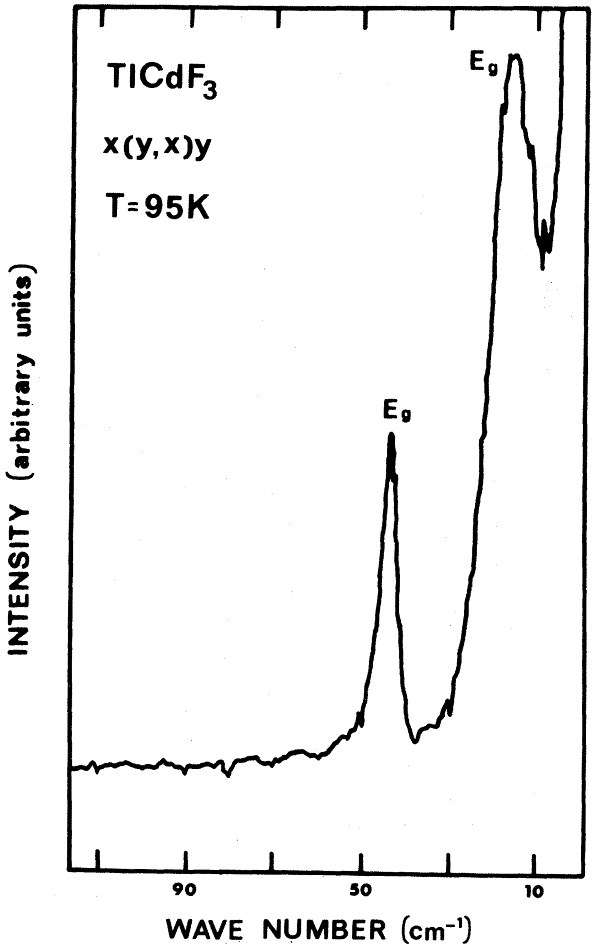

FIG. 10. Low-frequency Raman spectra of $TlCdF_3$ for E_g symmetry at 95 K.

that found in[11] $SrTiO_3$ and[12] $KMnF_3$ for which the R_{25} mode (when the origin is taken on an A^+ ion) which condensed to produce the transition splits into one soft mode of A_{1g} symmetry and another of E_g symmetry.

VII. SUMMARY

The first results we have obtained for these materials lead us to conclude that $RbCdF_3$ and $TlCdF_3$ undergo a phase transition associated with a soft mode at the R point of the cubic Brillouin zone. The corresponding order parameter is a rotation angle ϕ of the CdF_6 octahedra around $\langle 100\rangle$ pseudocubic axes. We would like to point out the interest of these compounds in the study of such antiferrodistorsive transitions. In fact, the quadratic phase is not affected by magnetic ordering as for $KMnF_3$, and the amplitude of the distortion is ten times larger than in $SrTiO_3$ (Fig. 12). So these compounds will be appropriate, for example, for accurate determination of critical exponents. It can be noticed on Fig. 12 that c/a varies linearly with T over a wide range of temperatures for $TlCdF_3$. It has been shown by Alefeld[13] that c/a is proportional to ϕ^2; thus a Landau-type behavior is assumed in this temperature range. Accurate values of critical exponents in the vicinity of T_c will be published later.

In order to complete our investigation, it will be desirable to study by inelastic neutron scattering the behavior of the mode of vibration associated with the R point of the cubic Brillouin zone for $T > T_c$. Unfortunately, owing to the great absorption of neutron by cadmium, it is quite impossible to carry out such experiments. Thus, we have begun to study an equivalent sequence of materials with Ca instead of Cd and particularly $RbCaF_3$ for which Δr_{AF} is largely positive ($\Delta r_{AF} = 0.096$). We have grown large single crystals of this compound available for ultrasonics, Raman scattering, and neutron scattering experiments. Our first x-ray measurements[14] show that a quadratic distortion with c/a greater than one occurs at 193 ± 1 K in $RbCaF_3$. This value disagrees slightly with $T_c = 198$ K, reported recently by Modine *et al.*[3]

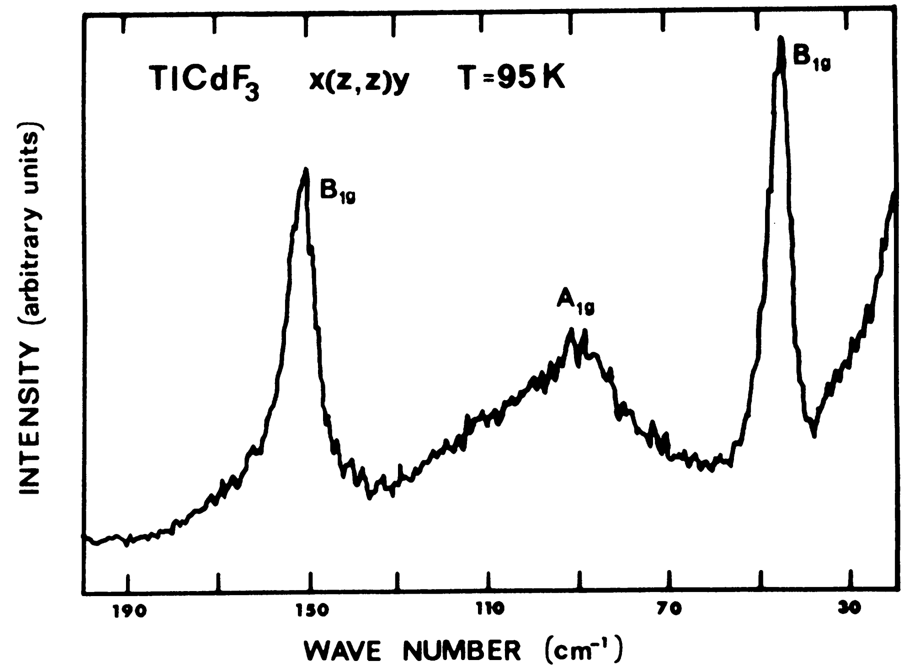

FIG. 11. Low-frequency Raman spectra of TlCdF$_3$ for zz polarization at 95 K.

ACKNOWLEDGMENTS

We thank N. Lenain, D. Simons, C. Carry, G. Hamel, and G. Niesseron for technical assistance.

APPENDIX

The electrostatic energy of an ion in a crystal is given by

$$U_i = \sum_j \frac{e^2 Z_i Z_j}{r_{ij}} .$$

In the perovskite structure, when taking as unit cell the cube of edge $R = \frac{1}{2}a$, every ion can be located with integer indices I, J, and K. Then

$$U_i = e^2 \sum_{I,J,K} \frac{A(I,J,K)}{(R^2I^2+R^2J^2+R^2K^2)^{1/2}} = -\alpha_i \frac{e^2}{R} ,$$

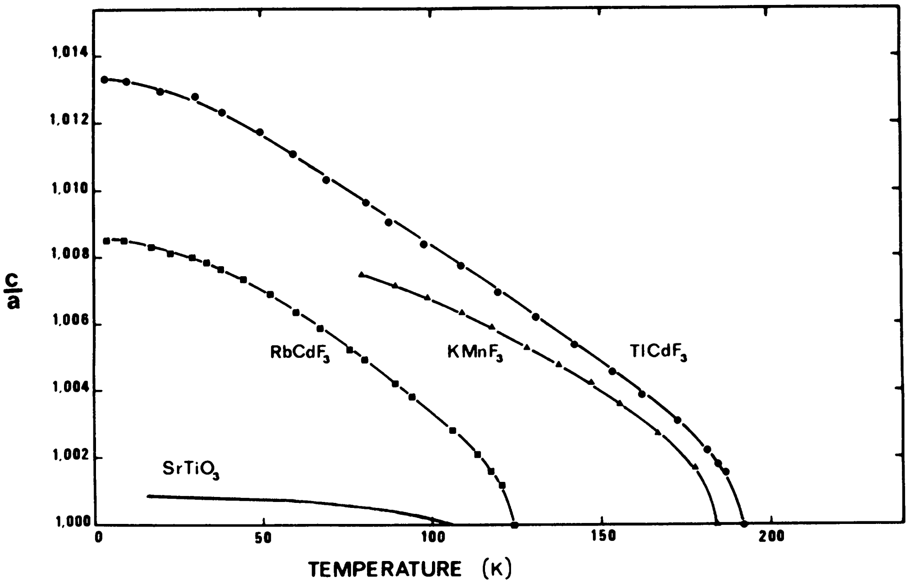

FIG. 12. Temperature variation of c/a in the quadratic phases of TlCdF$_3$, KMnF$_3$, RbCdF$_3$, and SrTiO$_3$. For SrTiO$_3$, the results are derived from the data of Okazaki and Kawaminami (Ref. 15).

where

$$\alpha_i = -\sum_{I,J,K} \frac{A(I,J,K)}{D} ,$$

with

$$D = (I^2 + J^2 + K^2)^{1/2} .$$

Let us displace ion i from its equilibrium position. The displacement is characterized by x, y, z $(x, y, z, \ll R)$. The electrostatic energy of the i ion is then given by

$$U_i' = -\alpha_i' e^2/R ,$$

where

$$\alpha_i' = -\sum_{I,J,K} \frac{A(I,J,K)}{[(I - x/R)^2 + (J - y/R)^2 + (K - z/R)^2]^{1/2}} .$$

α_i' may be written in the form

$$\alpha_i' = -\sum_{I,J,K} \frac{A(I,J,K)}{D[1 + (x^2 - 2IRx)/R^2D^2 + (y^2 - 2JRy)/R^2D^2 + (z^2 - 2KRz)/R^2D^2]^{1/2}} .$$

In the perovskite structure, since every ion is located at a center of symmetry, expanding α_i' with respect to x, y, and z, the first terms different from zero are

$$\alpha_i' = \alpha_i + M_x x^2/R^2 + M_y y^2/R^2 + M_z z^2/R^2 ,$$

where

$$M_x = -\sum_{I,J,K} A(I,J,K) \left(\frac{3}{2} \frac{I^2}{D^5} - \frac{1}{2D^3} \right) .$$

For an ion located in a site of cubic symmetry, $M_x = M_y = M_z = 0$. For a fluorine ion located in a site of symmetry D_{4h}, a computer calculation gives

$$M_x = \beta_{F\parallel} = 2.6768 , \quad M_y = M_z = \beta_{F\perp} = -1.3384 .$$

---

*Laboratoire associé au Centre National de la Recherche Scientifique No. 71.

[1] *Structural Phase Transitions and Soft Modes*, edited by E. J. Samuelsen, E. Andersen, and J. Feder (Universitetsforlaget, Oslo, 1971), and references therein.

[2] F. Denoyer, R. Comès, M. Lambert, and A. Guinier, Acta Crystallogr. A 30, 423 (1974).

[3] F. A. Modine, E. Sonder, W. P. Unruh, C. B. Finch, and R. D. Westbrook, Phys. Rev. B 10, 1623 (1974), and references therein.

[4] M. Rousseau, J. Y. Gesland, J. Julliard, J. Nouet, J. Zarembowitch, and A. Zarembowitch, J. Phys. Lett. 36, 121 (1975).

[5] A. M. Glazer, Acta Crystallog. B 28, 3384 (1972).

[6] R. A. Cowley, Phys. Rev. 134, 981 (1964); W. G. Stirling and R. A. Cowley, J. Phys. (Paris) 33, C2-135 (1972).

[7] M. Rousseau, J. Nouet, and A. Zarembowitch, J. Phys. Chem. 35, 921 (1974).

[8] J. Nouet, thesis (Paris VI University, 1973) (unpublished).

[9] R. D. Shannon and C. T. Prewitt, Acta Crystallogr. B 25, 925 (1969).

[10] J. Julliard and J. Nouet, Rev. Phys. Appl. (to be published).

[11] P. A. Fleury, J. F. Scott, and J. M. Worlock, Phys. Rev. Lett. 21, 16 (1968).

[12] Y. U. Popkov, V. Eremenko, and V. Fomin, Fiz. Tverd. Tela. 13, 2028 (1971) [Sov. Phys. Solid State 13, 1701 (1972)]; D. J. Lockwood and B. H. Torrie, J. Phys. C 7, 2729 (1974).

[13] B. Alefeld, Z. Phys. 222, 155 (1969).

[14] C. Ridou, J. Y. Gesland, M. Rousseau, J. Nouet, and A. Zarembowitch (unpublished).

[15] A. Okazaki and M. Kawaminami, Mater. Res. Bull. 8, 545 (1973).